Research Square

Preprints are preliminary reports that have not undergone peer review.
They should not be considered conclusive, used to inform clinical practice,
or referenced by the media as validated information.

Biogenic copper oxide nanomaterials development, characterization, antibacterial potential, antioxidant activity and in vitro toxicity estimation

Shruti Tyagi
WOS-B Scheme of DST, Noida Institute of Engineering and Technology
Arvind Kumar
Noida Institute of Engineering and Technology
Pankaj Kumar Tyagi (pktgenetics@gmail.com)
Noida Institute of Engineering and Technology

Research Article

Keywords: copper oxide nanoparticles, antibacterial potential, antioxidant activity, toxtrak test, in vitro toxicity, eco-friendly approach, sustainable synthesis of nanomaterials

Posted Date: May 30th, 2023

DOI: https://doi.org/10.21203/rs.3.rs-2992455/v1

License: This work is licensed under a Creative Commons Attribution 4.0 International License.
Read Full License

Abstract

This study describes the use of an extract from *Cassia fistula Linn* (Cf) leaves to produce biogenic copper oxide nanoparticles (CuONPs) employing a green synthesis approach. UV-Vis, FTIR, DLS, XRD and TEM studies are implemented to characterize the synthesized CfBio-CuONPs. A maximum peak was produced by the CfBio-CuONPs at 272 nm. The CfBio-CuONPs were crystalline, according to XRD measurements. The O-H group, aromatic group, and other functional groups were present in the FTIR spectrum of CfBio-CuONPs. The spherical, 15–25 nm-diameter CfBio-CuONPs were investigated using TEM to determine their size and shape. The antibacterial potential of the synthesized CfBio-CuONPs was then examined against four pathogenic bacteria *Escherichia coli*, *Pseudomonas aeruginosa*, *Staphylococcus epidermidis*, *Bacillus subtilis* and it was found that *E. coli* had the highest zone of inhibition (282.4), followed by *B. subtilis* (272.01), *P. aeruginosa* (240.97), and *S. epidermidis* (231.2). The maximum antioxidant activity (73% 1.54%) of CfBio-CuONPs was detected at a dose-dependent concentration of 2000 g/ml. On the other hand, the toxtrak test was used to determine the *in vitro* toxicity of CfBio-CuONPs and evaluate the percentage inhibition (%PI). According to the data, CfBio-CuONPs have a substantially stronger toxic effect value/PI against *E. coli* (93.52%) than against *P. aeruginosa* (92.65), *B. subtilis* (91.25%), and *S. epidermidis* (82.89%). These results also show that CfBio-CuONPs are more effective in killing harmful bacteria than antibiotics. Overall, the results of this study demonstrate that CfBio-CuONPs are superior to chloramphenicol and close to gentamycin in their ability to eliminate pathogenic microorganisms. The ecotoxicological consequences may benefit from these findings.

Introduction

Enhancing size-dependent characteristics including high bioavailability and large surface areas is the aim main of nanotechnology ((Tyagi 2016; Abbasi et al. 2023). Physical, chemical, and mechanical approaches can traditionally be used to create nanoparticles, but their high cost and toxicity have caused the fabrication of NPs to shift towards biological mechanisms (Kuberan et al. 2020; Lahiri et al. 2021). Bacteria are among the most desirable microorganisms to synthesize NPs because of their exceptional qualities, such as high stability, rapid generation, healthy conditions for investigation, relatively simple culture, resistance to the majority of hazardous heavy metals, and capacity for mass production of sustainable NPs (Mohd Yusof et al. 2019; Waris et al. 2021). CuONPs were to be synthesized efficiently and environmentally conscious, and their biological activity was to be evaluated. After screening a wide range of plants for synthesis of novel biogenic copper nanomaterial, we selected fresh leaves of *Cassia fistula Linn*. (Indian Laburnum) in order to achieve this goal. The flowering plant *Cassia fistula*, a member of the Fabaceae family, is sometimes referred to as the pudding-pipe tree, purging cassia, Indian laburnum. The species is native to Bangladesh, Myanmar, Thailand, and the Indian subcontinent, which extends from southern Pakistan to India and Sri Lanka to those nations. It is a stunning plant that serves a purpose in herbal medicine. After extract preparation, we go on to the synthesis of nanoparticles. Successfully synthesized nanoparticles were purified through centrifugation/filtration before being characterized. The UV-visible spectroscopy and Fourier transform infrared specified functional groupings

determined optical properties. X-ray diffraction studies of the crystallite sizes were combined with zeta potential measurements of surface charge and physical stability. A number of surface properties, such as shape and roughness, were examined using electron microscopy, and the hydrodynamic particle size was determined using dynamic light scattering. Following that, the broth micro dilution technique and the DPPH test were used to evaluate the antibacterial and antioxidant properties of CfBio-CuONPs. We employed a UV-Vis spectrophotometer, FTIR spectroscopy and DLS particle size analyzer (conducted by the host institute), and outsourced TEM and XRD for characterization (SAIF Institution facility AIIMS, New Delhi on payment bases).

Materials and Procedures

Chemicals

All of the chemicals and reagents used in this investigation were obtained from CDH and SRL without any additional purification.

Preparation of extract from C. fistula plant leaves

Fresh leaves of the *C. fistula* were properly cleansed to eliminate any contamination before being placed in distilled water (d.H_2O) to make the leaf extract. 10 g of the leaves from *C. fistula* were ground into a powder using a pestle and mortar. This powder was combined with 500 mL of d.H_2O and heated for 50 minutes at 80°C. Muslin cloth was used to filter the mixture before Whatman filter paper No. 1 was used. As a consequence, *C. fistula* leaf extracts in the color of red wine (ruby) were produced. These extracts were then kept at 4°C for future use.

Synthesis of CfBio-CuONPs

The extract solution from *C. fistula* plant leaf (75 mL) and copper chloride dihydrate solution (CuCl2•H2O) (1.34 g in 25 mL) were combined, and the mixture was agitated for an hour. If the mixing solution's color changed, that is the primary sign that CuONPs have formed. After being filtered and centrifuged, the produced solutions were examined by employing further nanoparticle characterization tools and techniques.

UV-vis spectroscopy

UV-VIS spectroscopy was used to examine the optical characteristics of CfBio-CuONPs (Shimadzu 1800). For evaluating the sample's spectral characteristics, a UV-vis spectrophotometer (Shimadzu UV-1800, Japan) was used to scan the samples between 200 and 800 nm ranges with a resolution of 1 nm.

FTIR spectroscopy

To identify the organic functional groups on CfBio-CuONPs, FTIR spectroscopy was employed. In the current investigation, potassium bromide (KBr) was mixed with the copper nanomaterial solutions to scan them in the 4,000 to 400 cm-1 wavenumber range. A KBr pellet was used as a reference.

XRD analysis

CfBio-CuONPs crystallinity was verified using XRD investigation (Nakhaeepour et al. 2019). To conduct the experiment, an X-ray diffractometer with Cu-K radiation (= 1.5418 A°) was employed. A 40 kV operating voltage, a 30 mA operating current, and a 0.2 s/step integration time were its operational specifications. The following formula was used to calculate the typical crystallite size: $d = 0.9 \lambda/\beta \cos \theta$

Where d is the average crystallite size, ß is the finish peak width at half maximum, λ is the wavelength of X-ray (1.5418 Å) and θ is the 2θ angle in peak.

DLS size analysis

Following a minor procedure change, as previously mentioned, the average size and stability of CfBio-CuONPs were evaluated under RT and at neutral pH (Sarkar et al. 2020). To determine the average size distribution, 100 g/ml of each sample was dissolved in ethanol and sonicated for 5 min. Following this, samples were assessed three times using a DLS analyzer.

TEM analysis

TEM samples have been obtained in accordance with the previously described technique (Ahuja et al. 2021; Ssekatawa et al. 2022) to explore the morphological and topological characteristics of CfBio-CuONPs. To do this, ethanol was used to disperse each sample at a concentration of 1 mg/ml, after which it was sonicated and put onto copper grid thin films. TEM operated at about 100 kV accelerating voltage was used to capture micrographs. Using ImageJ software, the sizes of 50 randomly selected particles from each sample were calculated to create the particle size distribution plots.

Antibacterial potential

The antibacterial activity of CfBio-CuONPs against pathogenic microbes such *E. coli, P. aeruginosa, S. epidermidis, and B. subtilis* was evaluated using a broth micro-dilution approach (Binesh et al. 2021). In nutrient broth, a suspension of pathogenic bacteria was prepared at a concentration of $1.5X10^8$ CFU/mL (0.5 McFarland standards). In order to determine the minimum inhibitory concentration (MIC), 100µl of CfBio-CuONPs were diluted successively (from 500 to 1.9µg/ml) and In 96-well plates with 100 µlof Muller-Hinton broth medium, 10 µl of pathogenic bacteria were added to each well. After that, the mixture was incubated for 18 hours at 37°C in an incubator shaker. Then, using a spectrophotometer (Shimadzu 1800), the absorbance at 630 nm was calculated. Muller-Hinton agar plates were incubated at 37°C for an additional 24 hours after 5 µl of each dilution was applied in order to determine the minimum bactericidal concentration (MBC).

Analysis of antioxidant activity

According to a previously published study (Barani et al. 2021), the antioxidant activity of CuONPs may be measured by their capacity to scavenge synthetic stable radicals of 2, 2-diphenyl-1-picrylhydrazyl (DPPH).

In order to achieve this, 96-well plates containing various concentrations of CfBio-CuONPs (31.2, 62.5, 125, 250, 500, and 1,000 µg/ml) were filled with 0.14 mM DPPH in methanol, and ascorbic acid was employed as a reference standard solution. The plates were then kept at 37°C for another 30 minutes of incubation. A spectrophotometer was used to measure the absorbance (A) at 517 nm, and the formula below was then applied to quantify the free radical scavenging activity of the

CfBio-CuONPs:

$$\text{DPPH radical scavenging activity } (\%) = \left(\frac{AS - (AT - AB)}{AS}\right) \times 100$$

Where AB stands for "absorbance of the blank wells," AS "absorbance of the standard solution," and AT "absorbance of the test wells"

In vitro **toxicity assessment of CfBio-CuONPs**

The *in vitro* toxicity of CfBio-CuONPs was assessed using the Toxtrak test technique of toxicity evaluation, as described by Tyagi et al. 2016 (Tyagi 2013; Tyagi et al. 2016; Liwarska-Bizukojc et al. 2016). The standard technique used in this experiment to determine cell viability is oxidation-reduction based on the resazurin dye (Bettaieb Rebey et al. 2012). To assess toxicity, use the dying of bacterial cells in suspension and the decrease of the resazurin dye with reacting synthesized nanoparticles. As a test sample of pathogenic bacteria *S. epidermidis, B. subtilis, E. coli, and P. aeruginosa* were mixed in a 25 g/mL solution in 12 broth culture tubes, 4 of which were filled with CfBio-CuONPs, while the other 4 were filled with a 1mL antibiotic suspension of chloramphenicol and rest 4 filled with a 1mL antibiotic suspension of gentamicin. Chloramphenicol and gentamicin were tagged with the AC_1 to AC_4 and AG_1 to AG_4, respectively, while *S. epidermidis, B. subtilis, E. coli, and P. aeruginosa* containing 4 culture tubes were labeled with the labels TS_1, TS_2, TS_3 and TS_4 respectively. A control sample was also run in the 4 additional test tubes and labeled with CS_1, CS_2, CS_3, and CS_4 each tubes containing only 25 g/mL broth suspension of *S. epidermidis, B. subtilis, E. coli*, and *P. aeruginosa*, respectively. Each culture tubes of all the three groups were provided 40µL of resazurin dye, and the tubes were incubated for 0 to 4 hours. All test tubes reading was taken in UV-spectrophotometer at 603nm which is specific for blue color. Subsequently, four readings were taken after one hour of interval.

The Toxtrak test is used for toxicity estimation as Percentage Inhibition (PI).

Percentage Inhibition = Δ A sample/ΔA control × 100

Where Δ A = Initial absorbance value − Final absorbance value

Statistical analysis

The data in this paper was analyzed using Statistica; release 7.0 StatSoft an advanced analytics software system.

Results and discussion

Characterization of (CfBio-CuONPs)

In this study, CuONP biosynthesis was accomplished as an effective, non-toxic method by using an extract of *Cassia fistula Linn* (Cf) leaves. The biological process (green synthesis) of nanoparticles begins by the presence of phytochemicals in the plant extract acting as capping agents and also contributes significantly as a reducing agent after being exposed to only the precursors without using any intermediate chemicals. It has been demonstrated that cellular macromolecules found in bacteria, such as enzymes and proteins, could trigger CuONPs to develop by changing copper ions into copper atoms (Nakhaeepour et al. 2019; Bandeira et al. 2020).

Color confirmation:

Extract from the leaves of the *C. fistula* plant was combined with copper chloride dihydrate solution, and the combination was stirred for an hour. The above-mentioned chemical combination results in a reddish brown (amber) tinged solution, which serves as primary evidence that CuONPs are being formed (Fig. 1B). It was then centrifuged and filtered. The filtrate has been stored in a freezer at 4°C for further use.

Spectroscopy

After the copper oxide nanoparticles were synthesized, the samples were examined with a UV-VIS spectrophotometer using wavelengths between 200 and 800 nm. The CfBio-CuONPs absorb between 250 and 350 nm range, while the aqueous copper sulphate solution absorbance is generally measured at 620 nm. The reduction of copper ions in the aqueous solution and the synthesis of CfBio-CuONPs are confirmed by the detection of the multiple peaks from 252 to 272nm (Fig. 1A **Inset)** with the maximum absorption peak at 272 nm and the absence of absorbance at 620 nm (Fig. 1). These results have been confirmed by evidence indicating that biogenic CuONPs have a UV-vis absorbance spectrum between 285 and 570 nm (Cheirmadurai et al. 2014; Duman et al. 2016). The removal of capping agents, an increase in crystallite size, and/or the aggregation of metal oxide NPs have all been proposed as potential causes of changes in the arrangement of the SPR peak (Tang et al. 2012; Kayani et al. 2015; Gharibshahi et al. 2017).

FTIR Analysis

FTIR analysis was used to determine the functional groups of phytochemicals in the *C. fistula* leaf extract that would be in charge of reducing copper ions to CfBio-CuONPs. Metal ions (Cu^{+}) are mostly converted into copper oxide nanoparticles by phytochemicals, in addition to serving as capping agents. Capping agents inhibit the aggregation of nanoparticles by controlling the stability and shape of NPs. In a leaf extract from *C. fistula*, peaks at 3251, 2175, 1719, 1596, 1472, 1370, 1197, 1088, 1053, 890, 791, and 718 cm^{-1} were discovered (data not given). These peaks are associated with complex hydrogen interactions between OH groups and free OH molecules, as well as C-H stretching, saturated hydrocarbons, COH

stretching vibrations, and C = C aromatic ring stretching vibrations were observed. Additionally, the CfBio-CuONPs FTIR spectra (Fig. 2) show a peak at 3333 cm^{-1}, which indicates the considerable stretching vibration of the O-H group of alcohols and phenols. The tiny signal at 2078 cm^{-1} represents molecules that contain C = N bonds as a result of stretching. The band at 1637 cm^{-1} revealed that the amide and ester groups were being stretched in the -C = O direction, whereas the peak at 1400 cm^{-1} was assigned to the (C = O) NH2 group. The bands at 1385 cm^{-1} and 1271 cm^{-1}, respectively, demonstrated the N-O bond of aromatic-nitro compounds and the C-O bond of aromatic-ethers. The absorption peak at 1108 cm^{-1} indicates the stretching vibration of the C-C group. The bands at 694 cm^{-1} of CuO nanoparticles reveal their vibrational modes (Fig. 2). The stretching bands from 600 to 668 cm^{-1} demonstrate copper oxide absorption, while the band at 1720 cm^{-1}, which is capped by oxidized-polyphenol compounds of the ketone functional group, suggests the production of –CuONPs (Shi et al. 2017; Muñoz-Escobar and Reyes-López 2020). The tiny peaks in the infrared spectrum observed at lower frequencies than 700 cm^{-1} are due to CuO vibrations. According to previous reports (Kouhkan et al. 2019; Ali et al. 2020; Kuberan et al. 2020), the organic functional groups encasing CuONPs were discovered. Studies using FTIR indicate, phenolic compounds in flavonoids may bind to metal, indicating that they may create metal nanoparticles to avoid agglomeration and stabilize the medium (Rapachi et al. 2023; Ritu et al. 2023). It is therefore conceivable that biological molecules play two distinct functions in the synthesis and stability of copper oxide nanoparticles in an aqueous medium.

DLS Analysis

The most often used method for figuring out how big nanoparticles are is DLS. The size distribution was in the 4–12 nm range. The polydispersity index (PDI) obtained from the examination of the particle size was 0.712. (Fig. 3).These findings acknowledge earlier studies on biogenic CuONPs (Nasrollahzadeh et al. 2015; Gu et al. 2018; Kouhkan et al. 2020; Sarkar et al. 2020) and confirmed the conclusions achieved from the DLS analysis.

XRD Analysis

Strong structural peaks and an examination of their crystallite size of < 100 nm suggested the finding that CfBio-CuONPs are nanocrystalline. Copper oxide nanoparticles biosynthesized from *C. fistula* leaf extract are depicted in Fig. 4 along with their XRD pattern, which was verified by distinctive peaks. The primary reflections of CfBio-CuONPs are shown by the strong diffraction peaks at (2θ) 33.05°, 35.98°, 38.99°, 48.78°, 53.75°, 58.89°, and 62.73°, 66.34°, and 68.10°, which correspond to the (110), (111), (200), (-202), (020), (202), (-113), (311) and (022) planes, respectively, which concurs with the work that was previously reported (Ahamed et al. 2014; Sivaraj et al. 2014; Sharma et al. 2015; Sathiyavimal et al. 2018). CfBio-CuONPs diffraction peaks show a typical monoclinic crystal structure free of impurities, demonstrating that they were made from copper oxide nanoparticles of the highest quality. Nordin and Shamsuddin identified comparable CuO-NP peak heights using a variety of plant extracts (Shamsuddin and Raja Nordin 2019).

TEM Imaging

The TEM examination offers precise morphological insights into the size and structure of CfBio-CuONPs. Figure 5 demonstrates how the CfBio-CuONPs are produced with a relatively excellent monodispersity and have almost spherical shapes with sizes between 15 and 25 nm and no agglomeration. Other researchers reached similar conclusions in their research on the bio inspired green synthesis of copper oxide nanoparticles from *Syzygium alternifolium* (Wt.) Walp. (Yugandhar et al. 2017), copper oxide and manganese oxide nanoparticles synthesis from watermelon seed shell extract (Ekinci et al. 2022)

Antibacterial effects of biogenic CfBio-CuONPs

Staphylococcus epidermidis and *Bacillus subtilis*, two gram-positive bacteria, and *Escherichia coli* and *Pseudomonas aeruginosa*, two gram-negative bacteria had been selected for investigating the antibacterial activities against CfBio-CuONPs (Table 1). The zone of inhibition was calculated in mm. *E. coli* (28 ± 2.4) > *B. subtilis* (27 ± 2.01) > *P. aeruginosa* (24 ± 0.97) > *S. epidermidis* (23 ± 1.2) was the zone of inhibition pattern (Fig. 6). CfBio-CuONPs inhibited the growth of *S. epidermidis* and *B. subtilis*, *P. aeruginosa*, and *E. coli* at 250, 250, 500, and 1000 µg/ml, respectively, in accordance with the measurement of MIC values. Additionally, MBC values of CfBio-CuONPs were 500 µg/ml for gram-negative bacteria and 250 µg/ml for gram-positive bacteria (Fig. 7). Our research shows that CfBio-CuONPs have the potential to be an efficient replacement for antibiotics that are currently on the market. Given that copper is known to reduce mitochondrial respiration and cause apoptosis, a number of causes may be responsible for the high toxicity of copper nanoparticles (Ruiz et al. 2021). Similar comparative results have been observed by investigators evaluating the antibacterial properties of copper nanoparticles (Ramyadevi et al. 2012; Usman et al. 2013; Keihan et al. 2017; Kumar et al. 2023; Saha et al. 2023)

Table 1
Antibacterial potential (Zone of inhibition, MIC and MBC) of dose-dependent concentration of CfBio-CuONPs and antibiotics against gram-negative and positive pathogenic bacteria

		Gram-negative bacteria		**Gram-positive bacteria**	
		E. coli	*P. aeruginosa*	*S. epidermidis*	*B. subtilis*
Chloramphenicol	Zone of inhibition (mm)	24.2 ± 1.6	25.1 ± 2.45	24.4 ± 1.07	26 ± 1.22
Gentamicin		27 ± 1.45	19.8 ± 1.09	22.8 ± 0.98	25.3 ± .18
CfBio-CuONPs		28 ± 2.4	24 ± 0.97	23 ± 1.2	27 ± 2.01
	MIC (µg/ml)	1000	500	250	250
	MBC(µg/ml)	500	500	250	250

Antioxidant activity of biogenic CfBio-CuONPs

In the current work, CfBio-CuONPs were assessed for their antioxidant activity, and the results showed that they scavenged DPPH radicals in a dose-dependent manner. When compared to ascorbic acid as a reference, which exhibited 100% antioxidant activity at the same concentration, the findings of the administration of 2000 µg/ml CfBio-CuONPs revealed 78% ±1.54% antioxidant activity (Fig. 8). At all concentrations, it was found that ascorbic acid and CfBio-CuONPs had significantly varying scavenging activities ($p < 0.001$). According to the studies of other professionals, copper oxide nanoparticles have a comparable pattern of antioxidant activity against DPPH (Dolati et al. 2023; Asif et al. 2023)

In vitro **toxicity assessment of CfBio-CuONPs**

Based on an evaluation of the inhibitory impact on bacterial respiration processes, the toxtrak approach, an analytical tool for toxicity identification, obtains its findings. Toxtrak investigates how bacterial respiration affects the redox-active dye resazurin reduction. Since the suppression of bacterial respirometric activity is the main objective of the Toxtrak test, the toxicity of the sample may be quickly determined calorimetrically by a decrease in the rate of resazurin reduction (Tripathi and Sirohi 2016). Toxtrak was used to calculate the toxicity of CfBio-CuONPs, as mentioned by other scientists in their work that were published in authoritative journals (Boulekbache-Makhlouf et al. 2013). After obtaining the PI, how much detrimental CfBio-CuONPs against pathogenic bacterial species is determined? The data shown in depict Fig. 9 clearly indicates that the PI of CfBio-CuONPs is much greater against *E. coli* (93.52%) > *P. aeruginosa* (92.65%) > *B. subtilis* (91.25%) > *S. epidermidis* (82.89%). On the other hands the PI of antibiotic chloramphenicol was found higher against *B. subtilis* (91.10%) > *P. aeruginosa* (90.55%) > *E. coli* (88.10%) > *S. epidermidis* (87.35%) whereas the PI of antibiotic gentamicin was found higher against *E. coli* (95.62%) > *B. subtilis* (91.15%) > *S. epidermidis* (83.65%) > *P. aeruginosa* (75.65%). Overall, the present results show that CfBio-CuONPs are more effective in killing pathogenic bacteria than either chloramphenicol or antibiotics that are nearby gentamycin.

Conclusion

A green synthesis method was used to synthesize the biogenic copper oxide nanoparticles. The synthesized CfBio-CuONPs have been evaluated by color, UV-Vis, FTIR, DLS, XRD, and TEM investigations. *E. coli* showed the greatest zone of inhibition when tested for antibacterial ability against four pathogenic bacteria, followed by *B. subtilis, P. aeruginosa, and S. epidermidis.* CfBio-CuONPs were shown to have the highest antioxidant activity at a dose-dependent concentration of 2000 g/ml. On the other hand, the percentage inhibition (%PI) was assessed using the toxtrak test, which was used to detect the *in vitro* toxicity. These findings further demonstrate that CfBio-CuONPs are superior to antibiotics in their ability to eliminate harmful microbes. Overall, this study's findings show that when it comes to killing pathogenic bacteria, CfBio-CuONPs are close to gentamycin and superior to chloramphenicol. These results might have positive effects on ecotoxicological outcomes.

Declarations

Acknowledgement

The author Shruti Tyagi gratefully acknowledges DST, Govt. of India, New Delhi (Project No. DST/WOS-B/HN-22/2021-Shruti (G) for funds. The authors also acknowledge the constant support from the Director of this Institute

Author contributions

Conceptualizing was done by Shruti Tyagi and Arvind Kumar, who also wrote the first drafting of the MS. Pankaj Kumar Tyagi oversaw the actual work and also edited it before it was published. Shruti Tyagi, Pankaj Kumar Tyagi, and Arvind Kumar did the statistical analysis on the data employed in this MS.

Funding

Author Shruti Tyagi received funding from DST, Govt. of India, New Delhi (Project No. DST/WOS-B/HN-22/2021-Shruti (G).

Competing interests

The authors have not disclosed any competing interests

References

1. Abbasi R, Shineh G, Mobaraki M, et al (2023) Structural parameters of nanoparticles affecting their toxicity for biomedical applications: a review. Journal of Nanoparticle Research 25:1–35. https://doi.org/10.1007/s11051-023-05690-w
2. Ahamed M, Alhadlaq HA, Khan MAM, et al (2014) Synthesis, characterization, and antimicrobial activity of copper oxide nanoparticles. Journal of Nanomaterials 2014:. https://doi.org/10.1155/2014/637858
3. Ahuja A, Tyagi PK, Tyagi S, et al (2021) Potential of Pueraria tuberosa (Willd.) DC. to rescue cognitive decline associated with BACE1 protein of Alzheimer's disease on Drosophila model: An integrated molecular modeling and in vivo approach. International Journal of Biological Macromolecules 179:586–600. https://doi.org/10.1016/j.ijbiomac.2021.03.032
4. Ali K, Saquib Q, Ahmed B, et al (2020) Bio-functionalized CuO nanoparticles induced apoptotic activities in human breast carcinoma cells and toxicity against Aspergillus flavus: An in vitro approach. Process Biochemistry 91:387–397. https://doi.org/10.1016/j.procbio.2020.01.008
5. Asif N, Ahmad R, Fatima S, et al (2023) Toxicological assessment of Phormidium sp. derived copper oxide nanoparticles for its biomedical and environmental applications. Scientific reports 13:6246. https://doi.org/10.1038/s41598-023-33360-3

6. Bandeira M, Giovanela M, Roesch-Ely M, et al (2020) Green synthesis of zinc oxide nanoparticles: A review of the synthesis methodology and mechanism of formation. Sustainable Chemistry and Pharmacy 15:. https://doi.org/10.1016/j.scp.2020.100223
7. Barani M, Masoudi M, Mashreghi M, et al (2021) Cell-free extract assisted synthesis of ZnO nanoparticles using aquatic bacterial strains: Biological activities and toxicological evaluation. International Journal of Pharmaceutics 606:. https://doi.org/10.1016/j.ijpharm.2021.120878
8. Bettaieb Rebey I, Bourgou S, Ben Slimen Debez I, et al (2012) Effects of Extraction Solvents and Provenances on Phenolic Contents and Antioxidant Activities of Cumin (Cuminum cyminum L.) Seeds. Food and Bioprocess Technology 5:2827–2836. https://doi.org/10.1007/s11947-011-0625-4
9. Binesh N, Farhadian N, Mohammadzadeh A (2021) Enhanced antibacterial activity of uniform and stable chitosan nanoparticles containing metronidazole against anaerobic bacterium of Bacteroides fragilis. Colloids and Surfaces B: Biointerfaces 202:. https://doi.org/10.1016/j.colsurfb.2021.111691
10. Boulekbache-Makhlouf L, Medouni L, Medouni-Adrar S, et al (2013) Effect of solvents extraction on phenolic content and antioxidant activity of the byproduct of eggplant. Industrial Crops and Products 49:668–674. https://doi.org/10.1016/j.indcrop.2013.06.009
11. Cheirmadurai K, Biswas S, Murali R, Thanikaivelan P (2014) Green synthesis of copper nanoparticles and conducting nanobiocomposites using plant and animal sources. RSC Advances 4:19507–19511. https://doi.org/10.1039/c4ra01414f
12. Dolati M, Tafvizi F, Salehipour M, et al (2023) Biogenic copper oxide nanoparticles from Bacillus coagulans induced reactive oxygen species generation and apoptotic and anti-metastatic activities in breast cancer cells. Scientific Reports 13:1–19. https://doi.org/10.1038/s41598-023-30436-y
13. Duman F, Ocsoy I, Kup FO (2016) Chamomile flower extract-directed CuO nanoparticle formation for its antioxidant and DNA cleavage properties. Materials Science and Engineering C 60:333–338. https://doi.org/10.1016/j.msec.2015.11.052
14. Ekinci A, Kutluay S, Şahin Ö, Baytar O (2022) Green synthesis of copper oxide and manganese oxide nanoparticles from watermelon seed shell extract for enhanced photocatalytic reduction of methylene blue. International Journal of Phytoremediation. https://doi.org/10.1080/15226514.2022.2109588
15. Gharibshahi L, Saion E, Gharibshahi E, et al (2017) Structural and optical properties of ag nanoparticles synthesized by thermal treatment method. Materials 10:402. https://doi.org/10.3390/ma10040402
16. Gu H, Chen X, Chen F, et al (2018) Ultrasound-assisted biosynthesis of CuO-NPs using brown alga Cystoseira trinodis: Characterization, photocatalytic AOP, DPPH scavenging and antibacterial investigations. Ultrasonics Sonochemistry 41:109–119. https://doi.org/10.1016/j.ultsonch.2017.09.006
17. Kayani ZN, Saleemi F, Batool I (2015) Effect of calcination temperature on the properties of ZnO nanoparticles. Applied Physics A: Materials Science and Processing 119:713–720. https://doi.org/10.1007/s00339-015-9019-1

18. Keihan AH, Veisi H, Veasi H (2017) Green synthesis and characterization of spherical copper nanoparticles as organometallic antibacterial agent. Applied Organometallic Chemistry 31:e3642. https://doi.org/10.1002/aoc.3642
19. Kouhkan M, Ahangar P, Babaganjeh LA, et al (2020) Biosynthesis of copper oxide nanoparticles using Lactobacillus casei subsp. casei and its anticancer and antibacterial activities. ingentaconnect.com 16:101–111. https://doi.org/10.2174/1573413715666190318155801
20. Kouhkan M, Ahangar P, Babaganjeh LA, Allahyari-Devin M (2019) Biosynthesis of Copper Oxide Nanoparticles Using Lactobacillus casei Subsp. Casei and its Anticancer and Antibacterial Activities. Current Nanoscience 16:101–111. https://doi.org/10.2174/1573413715666190318155801
21. Kuberan R, Yadav SA, Sivaperumal S, et al (2020) Phytosynthesis and Characterization of Copper Oxide Nanoparticles using the Aqueous Extract of Beta vulgaris L and Evaluation of their Antibacterial and Anticancer. Springer 31:221–230. https://doi.org/10.1007/s10876-019-01640-6
22. Kumar M, Kaushik D, Kumar A, et al (2023) Anti obesity and antibacterial activity of green synthesis of copper nanoparticles by Nigella sativa seeds . International Journal of Food Science & Technology 58:2883–2892. https://doi.org/10.1111/ijfs.16359
23. Lahiri D, Nag M, Sheikh HI, et al (2021) Microbiologically-Synthesized Nanoparticles and Their Role in Silencing the Biofilm Signaling Cascade. Frontiers in Microbiology 12:. https://doi.org/10.3389/fmicb.2021.636588
24. Liwarska-Bizukojc E, Ślęzak R, Klink M (2016) Study on wastewater toxicity using ToxTrak^{TM} method. Environmental Science and Pollution Research 23:9105–9113. https://doi.org/10.1007/s11356-016-6096-4
25. Mohd Yusof H, Mohamad R, Zaidan UH, Abdul Rahman NA (2019) Microbial synthesis of zinc oxide nanoparticles and their potential application as an antimicrobial agent and a feed supplement in animal industry: A review. Journal of Animal Science and Biotechnology 10:. https://doi.org/10.1186/s40104-019-0368-z
26. Muñoz-Escobar A, Reyes-López SY (2020) Antifungal susceptibility of Candida species to copper oxide nanoparticles on polycaprolactone fibers (PCL-CuONPs). PLoS ONE 15:e0228864. https://doi.org/10.1371/journal.pone.0228864
27. Nakhaeepour Z, Mashreghi M, Matin MM, et al (2019) Multifunctional CuO nanoparticles with cytotoxic effects on KYSE30 esophageal cancer cells, antimicrobial and heavy metal sensing activities. Life Sciences 234:. https://doi.org/10.1016/j.lfs.2019.116758
28. Nasrollahzadeh M, Sajadi SM, Rostami-Vartooni A, Bagherzadeh M (2015) Green synthesis of Pd/CuO nanoparticles by Theobroma cacao L. seeds extract and their catalytic performance for the reduction of 4-nitrophenol and phosphine-free Heck coupling reaction under aerobic conditions. Journal of Colloid and Interface Science 448:106–113. https://doi.org/10.1016/j.jcis.2015.02.009
29. Ramyadevi J, Jeyasubramanian K, Marikani A, et al (2012) Synthesis and antimicrobial activity of copper nanoparticles. Materials Letters 71:114–116. https://doi.org/10.1016/j.matlet.2011.12.055

30. Rapachi D, Carlos CR, Pavan FA, Gelesky MA (2023) Metallic Nanoparticles Biosynthesized by Phenolic-Rich Extracts: Interaction, Characterization and Application. Journal of Cluster Science 1–15. https://doi.org/10.1007/s10876-023-02426-7
31. Ritu, Verma KK, Das A, Chandra P (2023) Phytochemical-Based Synthesis of Silver Nanoparticle: Mechanism and Potential Applications. BioNanoScience 2023 1–22. https://doi.org/10.1007/S12668-023-01125-X
32. Ruiz LM, Libedinsky A, Elorza AA (2021) Role of Copper on Mitochondrial Function and Metabolism. Frontiers in Molecular Biosciences 8:. https://doi.org/10.3389/fmolb.2021.711227
33. Saha T, Bin Mobarak M, Uddin MN, et al (2023) Biogenic synthesis of copper oxide (CuO) NPs exploiting Averrhoa carambola leaf extract and its potential antibacterial activity. Materials Chemistry and Physics 305:127979. https://doi.org/10.1016/J.MATCHEMPHYS.2023.127979
34. Sarkar J, Chakraborty N, Chatterjee A, et al (2020) Green synthesized copper oxide nanoparticles ameliorate defence and antioxidant enzymes in Lens culinaris. Nanomaterials 10:. https://doi.org/10.3390/nano10020312
35. Sathiyavimal S, Vasantharaj S, Bharathi D, et al (2018) Biogenesis of copper oxide nanoparticles (CuONPs) using Sida acuta and their incorporation over cotton fabrics to prevent the pathogenicity of Gram negative and Gram positive bacteria. Journal of Photochemistry and Photobiology B: Biology 188:126–134. https://doi.org/10.1016/j.jphotobiol.2018.09.014
36. Shamsuddin M, Raja Nordin N (2019) Biosynthesis of copper(II) oxide nanoparticles using Murayya koeniggi aqueous leaf extract and its catalytic activity in 4-nitrophenol reduction. Malaysian Journal of Fundamental and Applied Sciences 15:218–224. https://doi.org/10.11113/mjfas.v15n2.1390
37. Sharma JK, Akhtar MS, Ameen S, et al (2015) Green synthesis of CuO nanoparticles with leaf extract of Calotropis gigantea and its dye-sensitized solar cells applications. Journal of Alloys and Compounds 632:321–325. https://doi.org/10.1016/j.jallcom.2015.01.172
38. Shi LB, Tang PF, Zhang W, et al (2017) Green synthesis of CuO nanoparticles using Cassia auriculata leaf extract and in vitro evaluation of their biocompatibility with rheumatoid arthritis macrophages (RAW 264.7). Tropical Journal of Pharmaceutical Research 16:185–192. https://doi.org/10.4314/tjpr.v16i1.25
39. Sivaraj R, Rahman PKSM, Rajiv P, et al (2014) Biosynthesis and characterization of Acalypha indica mediated copper oxide nanoparticles and evaluation of its antimicrobial and anticancer activity. Spectrochimica Acta - Part A: Molecular and Biomolecular Spectroscopy 129:255–258. https://doi.org/10.1016/j.saa.2014.03.027
40. Ssekatawa K, Byarugaba DK, Angwe MK, et al (2022) Phyto-Mediated Copper Oxide Nanoparticles for Antibacterial, Antioxidant and Photocatalytic Performances. Frontiers in Bioengineering and Biotechnology 10:1. https://doi.org/10.3389/fbioe.2022.820218
41. Tang ZX, Fang XJ, Zhang ZL, et al (2012) Nanosize MgO as antibacterial agent: Preparation and characteristics. Brazilian Journal of Chemical Engineering 29:775–781. https://doi.org/10.1590/S0104-66322012000400009

42. Tripathi A, Sirohi R (2016) Antimicrobial activities of silver nanoparticles synthesized from peel of fruits and vegetables. Biological Insights 1:29–34
43. Tyagi K (2013) Estimation of toxic effects of chemically and biologically synthesized silver nanoparticles on human gut microflora containing Bacillus subtilis. Journal of Toxicology and Environmental Health Sciences 5:172–177. https://doi.org/10.5897/jtehs2013.0271
44. Tyagi PK (2016) Production of Metal Nanoparticles from Biological Resources. International Journal of Current Microbiology and Applied Sciences 5:548–558. https://doi.org/10.20546/ijcmas.2016.503.064
45. Tyagi PK, Mishra M, Khan N, et al (2016) Toxicological study of silver nanoparticles on gut microbial community probiotic. Environmental Nanotechnology, Monitoring and Management 5:36–43. https://doi.org/10.1016/j.enmm.2016.01.003
46. Usman MS, El Zowalaty ME, Shameli K, et al (2013) Synthesis, characterization, and antimicrobial properties of copper nanoparticles. International Journal of Nanomedicine 8:4467–4479. https://doi.org/10.2147/IJN.S50837
47. Waris A, Din M, Ali A, et al (2021) A comprehensive review of green synthesis of copper oxide nanoparticles and their diverse biomedical applications. Inorganic Chemistry Communications 123:. https://doi.org/10.1016/j.inoche.2020.108369
48. Yugandhar P, Vasavi T, Uma Maheswari Devi P, Savithramma N (2017) Bioinspired green synthesis of copper oxide nanoparticles from Syzygium alternifolium (Wt.) Walp: characterization and evaluation of its synergistic antimicrobial and anticancer activity. Applied Nanoscience (Switzerland) 7:417–427. https://doi.org/10.1007/S13204-017-0584-9/FIGURES/10

Figures

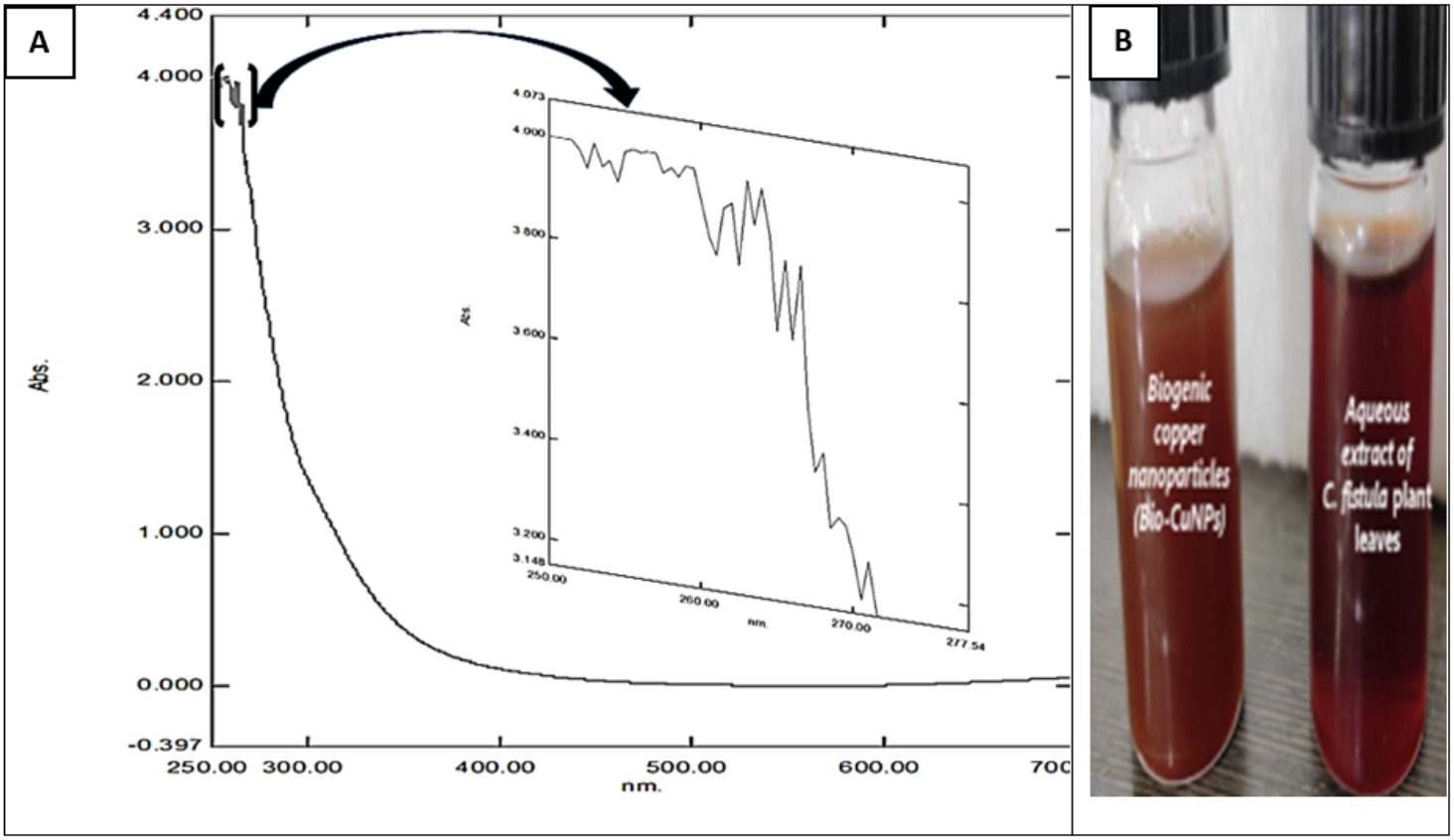


Figure 1

UV-visible absorption spectrum confirming the presence of CfBio-CuONPs (A), a reddish brown (amber) tinged solution is primary confirmation the formation of CuONPs (B).

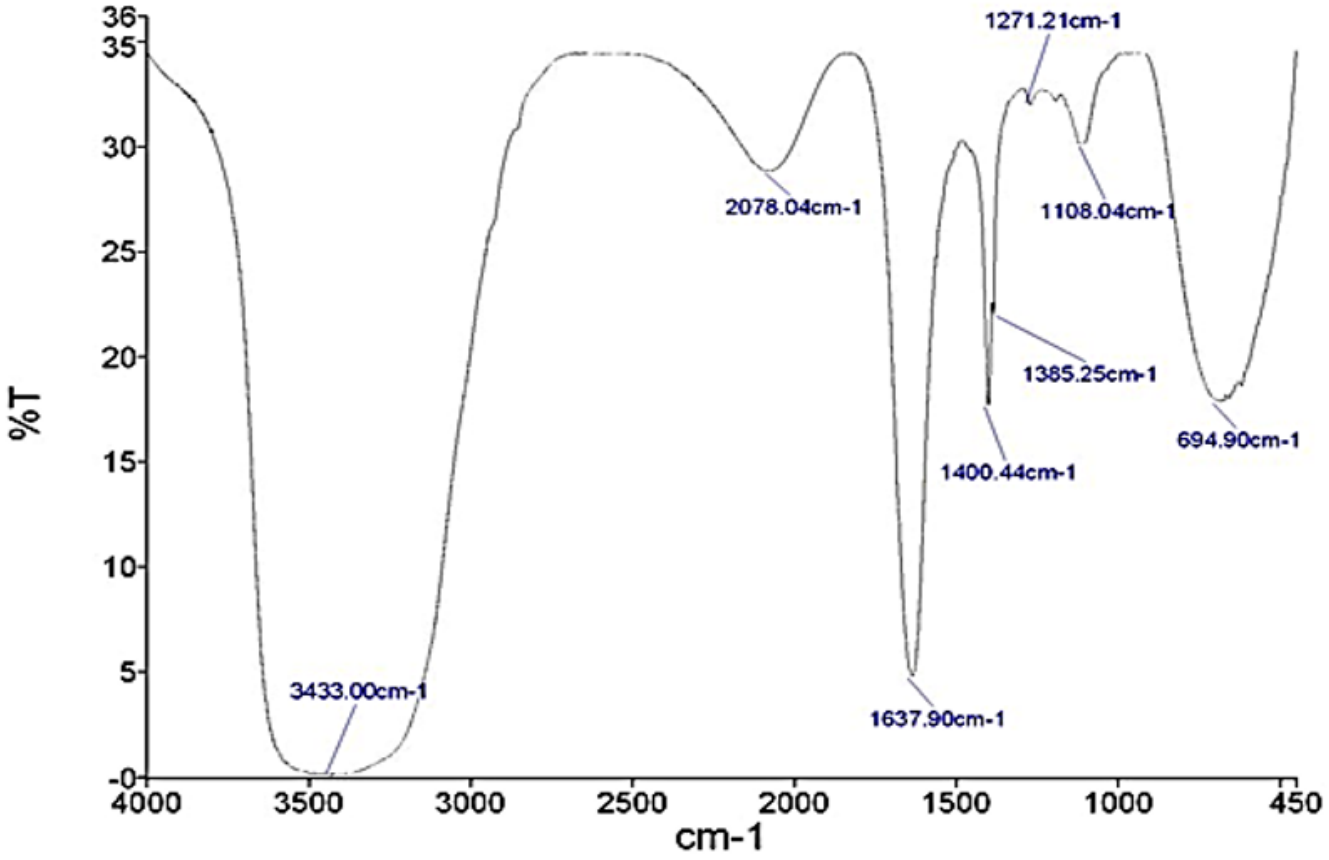


Figure 2

The CfBio-CuONPs synthesis functional groups are shown by an FTIR pattern.

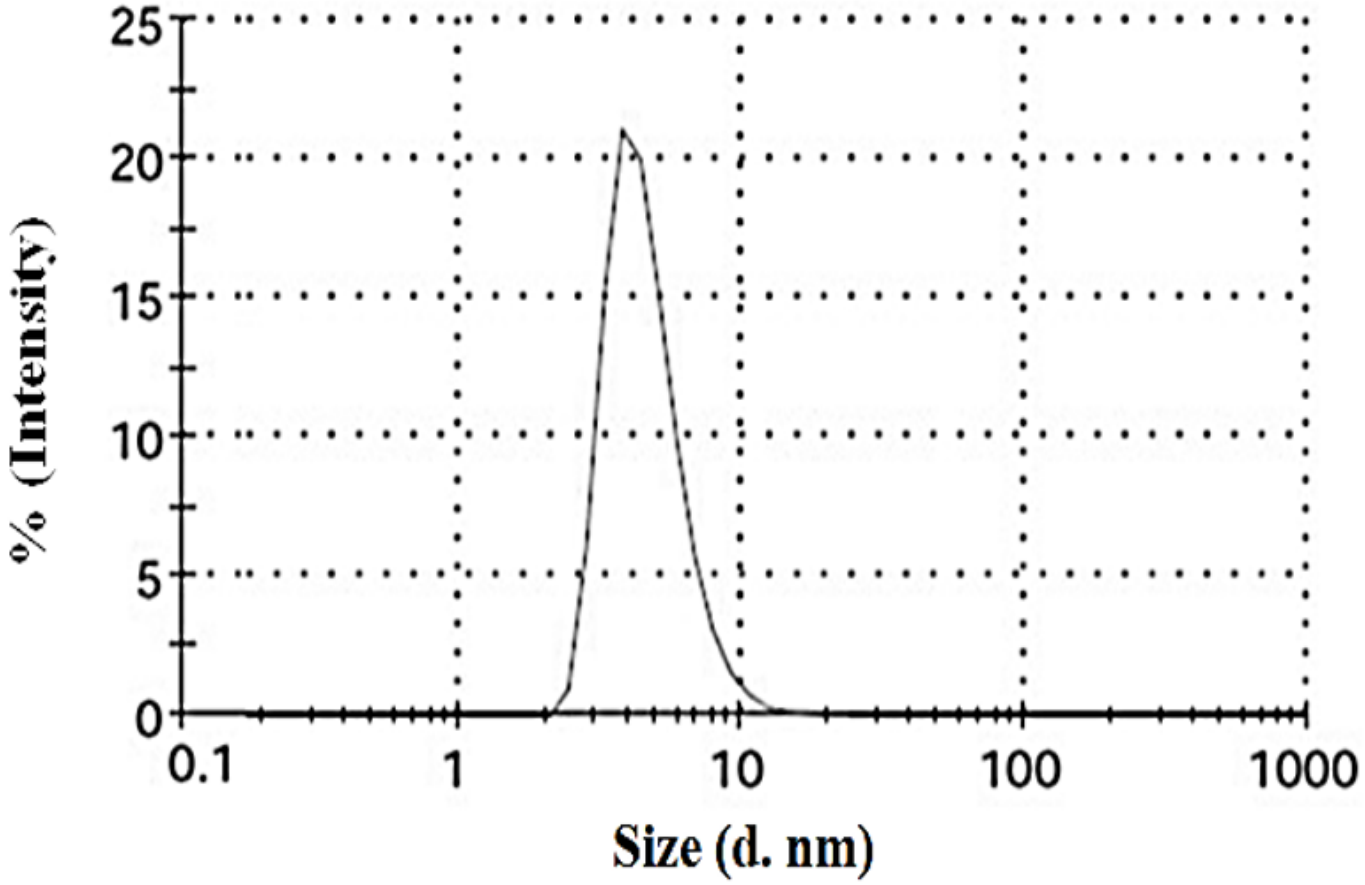


Figure 3

DLS indicating average size of Cassia fistula mediated CfBio-CuONPs

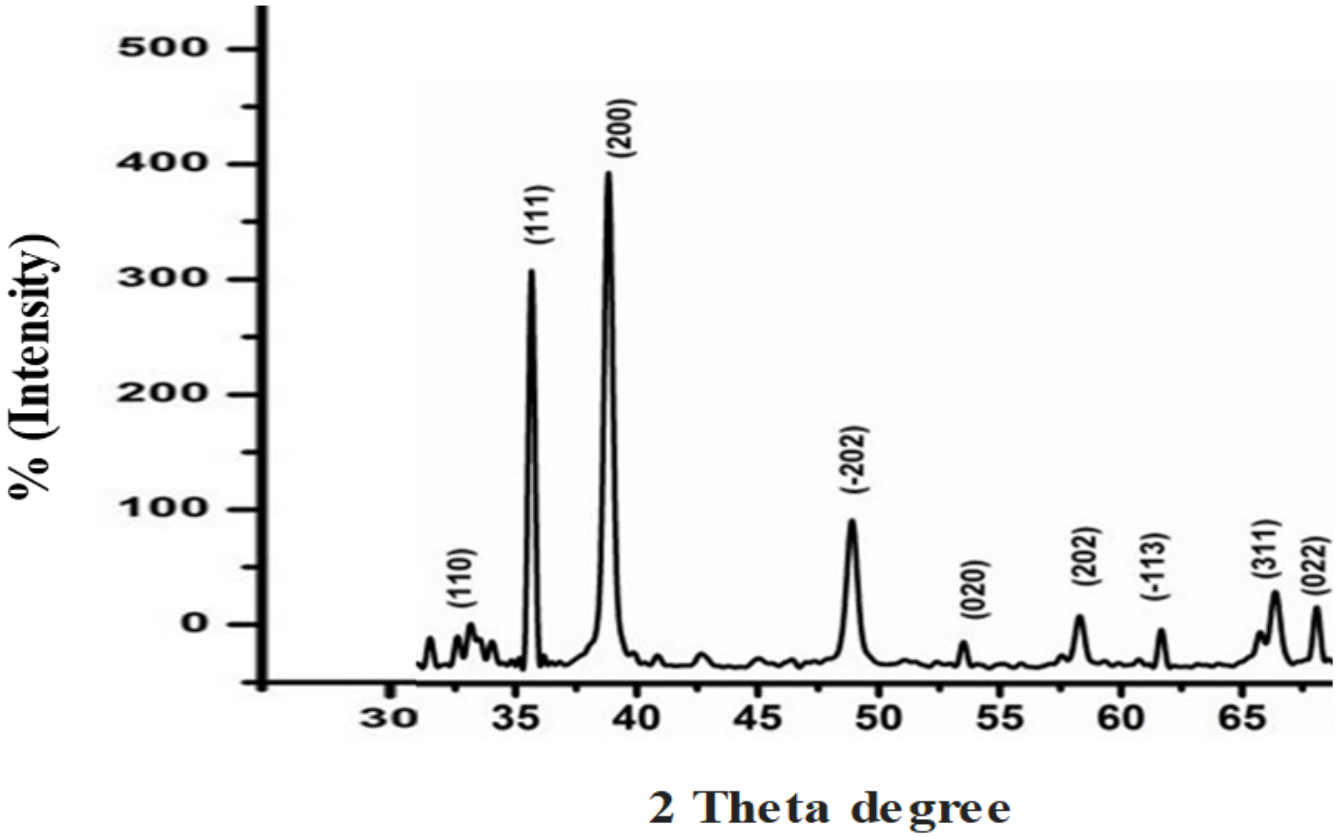


Figure 4

XRD pattern indicating presence of Cu peaks in CfBio-CuONPs suspension

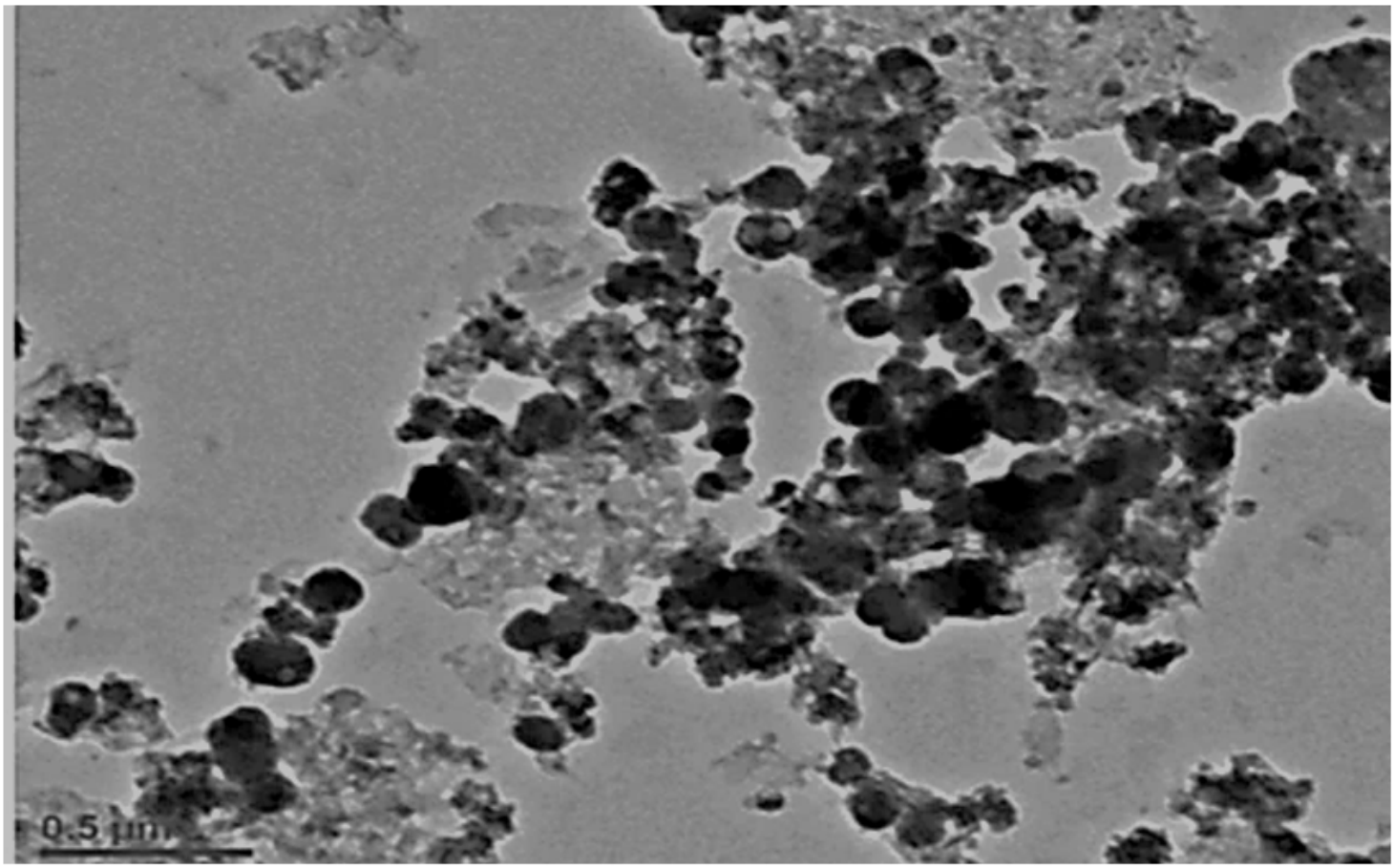


Figure 5

Transmission electron microscopic image of CfBio-CuONPs

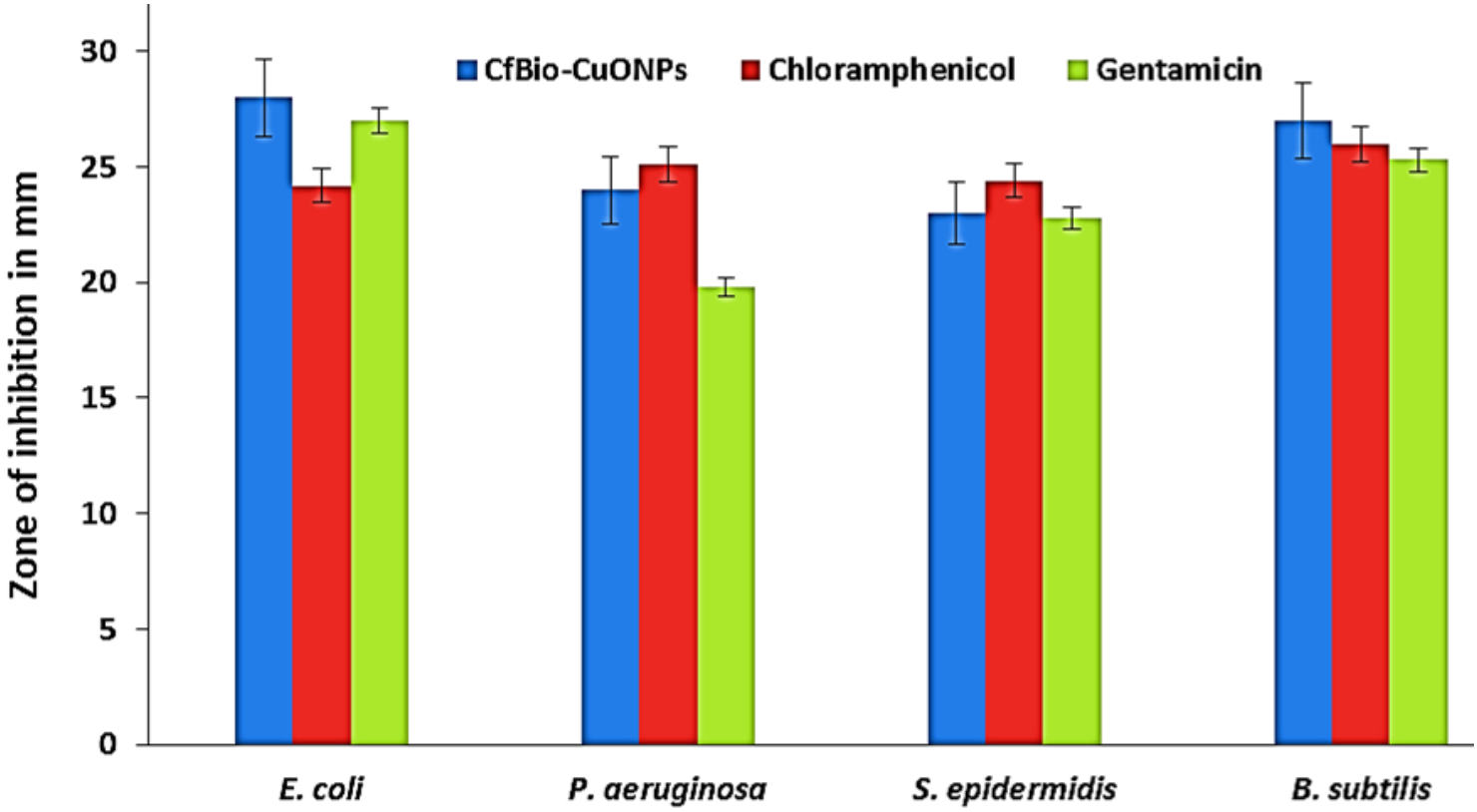
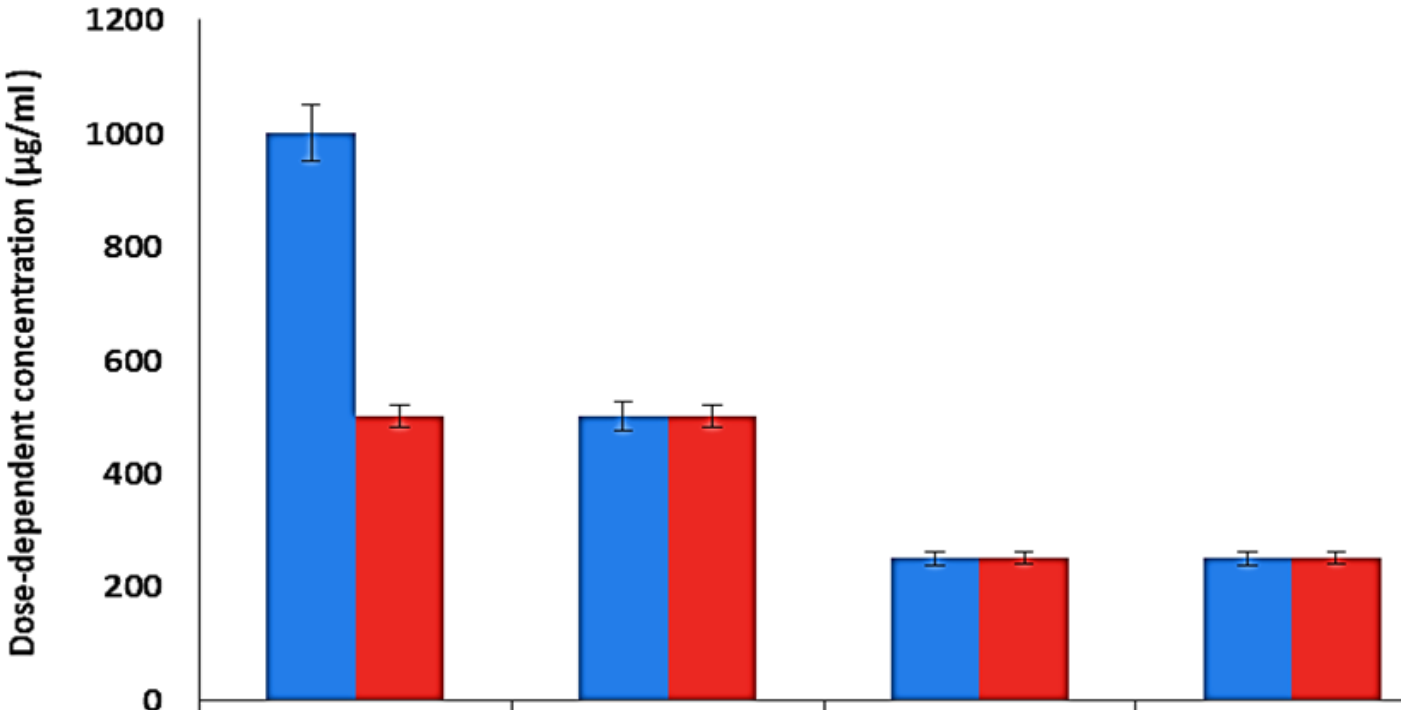


Figure 6

Antibacterial potential (Zone of inhibition in mm) of CfBio-CuONPs and antibiotics against pathogenic bacteria



	E. coli	P. aeruginosa	S. epidermidis	B. subtilis
MIC (µg/ml)	1000	500	250	250
MBC (µg/ml)	500	500	250	250

Figure 7

Antibacterial potential (MIC and MBC) of dose-dependent concentration of CfBio-CuONPs against pathogenic bacteria

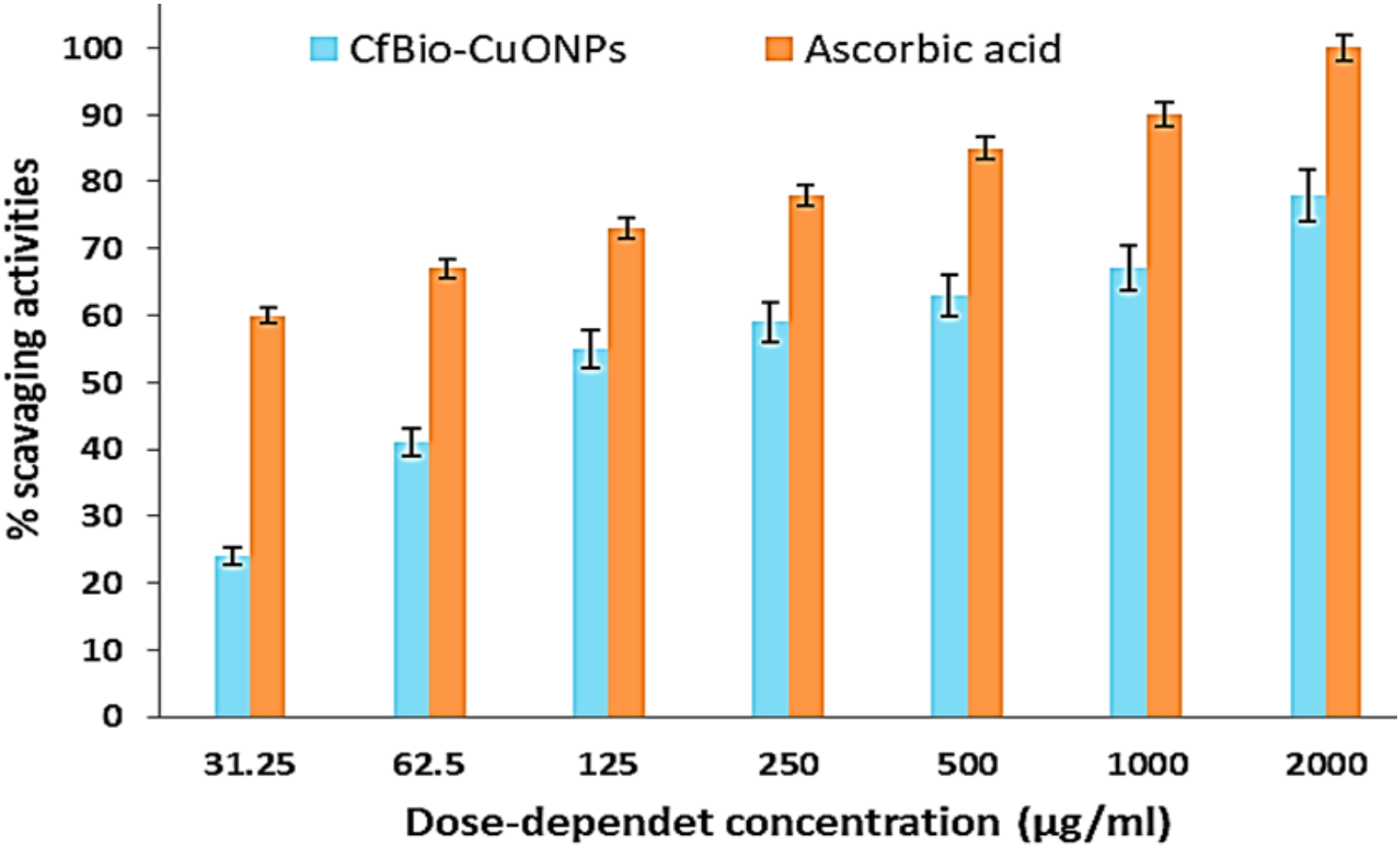
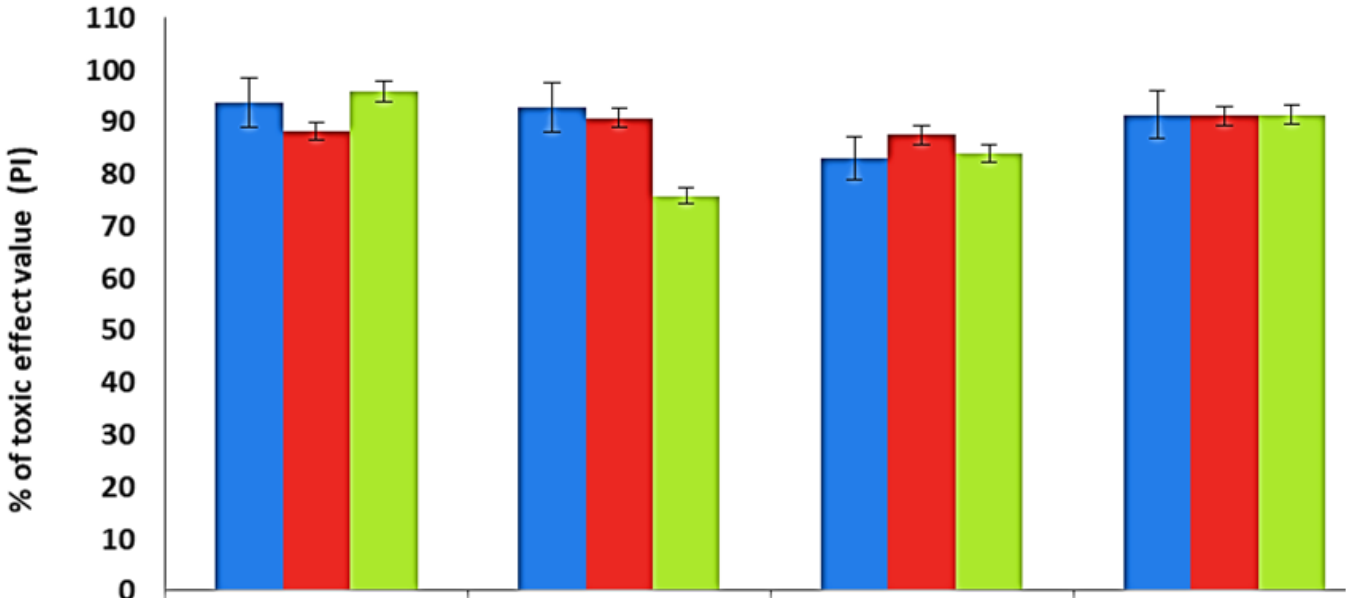


Figure 8

To calculate the antioxidant assay, there is a relationship between the dose-dependent concentration of CfBio-CuONPs, ascorbic acid, and% scavenging activity



	E. coli	P. aeruginosa	S. epidermidis	B. subtilis
CfBio-CuONPs	93.52	92.65	82.89	91.25
Chloramphenicol	88.1	90.55	87.35	91.1
Gentamicin	95.62	75.65	83.65	91.15

Figure 9

To calculate the *in vitro* toxicity (toxic effect value/% PI), of CfBio-CuONPs and antibiotics, against pathogenic bacteria

Supplementary Files

This is a list of supplementary files associated with this preprint. Click to download.

- graphicalabstract.jpg